

# Binary and Long-Term (Triple?) Modulations of 4U 1820–30 in NGC 6624

Y. Chou and J. E. Grindlay

*Harvard-Smithsonian Center for Astrophysics,  
60 Garden Street, Cambridge, MA 02138  
yichou@cfa.harvard.edu*

## ABSTRACT

We present timing analysis results for Rossi x-ray Timing Explorer (RXTE) observations of x-ray binary source 4U 1820–30 located in the globular cluster NGC 6624. The light curves of observations made between October 1996 and September 1997 show that the maximum of the 685s binary period modulation folded by the linear ephemeris from previous observations has phase shift of  $-0.20 \pm 0.06$ . Combined with historical results (1976-1997), the binary period derivative is measured to be  $\dot{P}/P = (-3.47 \pm 1.48) \times 10^{-8} \text{ yr}^{-1}$ . The previous known ( $\sim 176$  d) long-term modulation is significant in the x-ray light curve obtained by analysis of the RXTE All-Sky Monitor (ASM) during the years 1996-2000. The RXTE/ASM ephemeris is extended by analysis of all historical data (Vela 5B and Ginga) to yield a period  $171.033 \pm 0.326$  days with no evidence for period change ( $|\dot{P}/P| < 2.20 \times 10^{-4} \text{ yr}^{-1}$ ). All reported x-ray burst activity is confined to within  $\pm 23$  d of the predicted minima. This stable long-term modulation is consistent with 4U 1820–30 being a hierarchical triple system with a  $\sim 1.1$  d period companion.

*Subject headings:* accretion, accretion disks — stars individual (4U 1820–30) — x-rays stars

## 1. INTRODUCTION

The low-mass x-ray binary (LMXB) 4U 1820–30 near the center of the globular cluster NGC 6624 (Grindlay et al. 1984) has a binary orbital period of 685.0118 sec (Stella, Priedhorsky & White 1987; Smale, Mason & Mukai 1987; Morgan, Remillard & Garcia 1988; Sansom et al. 1989; Tan et al. 1991; van der Klis et al. 1993a,b) and was the first x-ray burster identified with a known x-ray source (Grindlay et al. 1976). Its short orbital period

and its x-ray burst activity imply it is a system with a  $0.06\text{--}0.08 M_{\odot}$  helium white dwarf secondary star accreting mass onto a primary neutron star (Rappaport et al. 1987). A 176 d period long-term variation between high-luminosity and low-luminosity by factor of  $\sim 3$  was observed by the Vela 5B spacecraft (Priedhorsky & Terrell 1984, hereafter PT84). Quasi-periodic oscillations (QPO) with various frequencies were also reported (Stella, White & Priedhorsky 1987; Hasinger & van der Klis 1989; Smale, Zhang & White 1997; Zhang et al. 1998; Wijnands, van der Klis & Rijkhorst 1999; Kaaret et al. 1999).

Whereas the x-ray observations show an 11 minutes sinusoidal-like, small amplitude ( $\sim 3\%$  peak to peak) modulation, Anderson et al. (1997) discovered a large  $\sim 16\%$  (peak to peak) modulation (period  $687.6 \pm 2.4$  sec) in the UV band (wavelength in the 126–251 nm range) from the Hubble Space Telescope (HST). The modulation may come from the variable thickness of the outer disk rim (Stella, Priedhorsky & White 1987). The stability of the period ( $\dot{P}/P = (-5.3 \pm 1.1) \times 10^{-8} \text{ yr}^{-1}$ , van der Klis et al. 1993b) makes it certain that the 685 sec modulation is the orbital period. However, the negative period derivative is inconsistent with the lower limit ( $\dot{P}/P > +8.8 \times 10^{-8}$  per year) of the standard scenario proposed by Rappaport et al. (1987).

The 4U 1820–30 luminosity variation was first discovered by Canizares and Neighbours (1975) and its possible  $\sim 176$  d periodicity was first reported by PT84. The fact that x-ray bursts have only been seen in the low luminosity state (Clark et al. 1977, Stella, Kahn & Grindlay 1984) indicates that the long-term modulation is an intrinsic change in the accretion rate rather than an extrinsic absorption. However, significant phase shifts from the expected minima predicted by the ephemeris of the  $176.4 \pm 1.3$  d period proposed by PT84 have been observed from the EXOSAT (Haberl et al. 1987) and Ginga (Sansom et al. 1989). The  $\sim 176$  d periodicity, if stable, of the luminosity variation implies (Grindlay 1988) that 4U 1820–30 may be a hierarchical triple in which a third companion star with a period of  $\sim 1.1$  d orbits the 11 minute binary and thereby induces an inner binary eccentricity precession (Mazeh and Shaham, 1979) with a period of  $\sim 176$  d.

In this paper, we describe our RXTE 1996–1997 PCA and 1996–2000 ASM observations of 4U 1820–30 (section 2) and report the timing analysis of the data (section 3), including the 11 minute binary periodicity, phase jitter, period stability, updated quadratic ephemeris, and search for the  $\sim 1.1$  d period that could be associated with a third companion. Analysis of RXTE ASM data gives a new “176 d” modulation ephemeris which connects all the observations from 1969 to 2000 and exhibits no significant period derivative. In section 4, we discuss possible models for the observed light curve behavior of 4U 1820–30.

## 2. RXTE OBSERVATIONS

The RXTE PCA/HEXTE pointed observations of 4U 1820–30 were made on 1996 October 26, 28 and 30, and at least once per month between 1997 February and September. The observation time interval spanned about two 176 d luminosity cycles. Details of the RXTE PCA/HEXTE observations are listed in Table 2 in Bloser et al. 2000. The data used for the analysis are in PCA (PCU 0 and 1) Standard-2 format with a time resolution of 16 sec. We divide the data into 4 energy bands, 1.72–3.18 keV, 3.18–5.01 keV, 5.01–6.84 keV and 6.84–19.84 keV. Since our timing analysis did not suggest any significant energy dependence of the patterns observed, we will present in this paper only the analysis results for band 4 (6.84–19.84 keV) unless otherwise specified. A typical PCA Standard-2 light curve is shown in Figure 1. A complete analysis of the spectra and spectral variations of 4U 1820–30 for these RXTE observations is presented by Bloser et al. (2000).

Data for the 4U 1820–30 RXTE/ASM x-ray light curve (2–12 keV) analyzed in this paper were collected from 1996 January 11 to 2000 March 2 (Figure 2). The observation window (1576 days) spanned about 9 contiguous 176 d modulation cycles. In each modulation cycle, the count rate varies from  $\sim 5$  to  $\sim 35$  counts/sec.

## 3. DATA ANALYSIS

### 3.1. Binary Periodicity and Phase Analysis

All RXTE PCA data were first corrected for the barycenter arrival times. In order to avoid the possible alias from the  $\sim 176$  d period long-term modulation, we removed the DC term from the observed light curve. We carried out a  $\chi^2$  analysis of the folded light curves (32 bins per period) to search for the best period near 685 sec for the entire 4U 1820–30 RXTE PCA data. The maximum  $\chi^2$  (deviation of folded light curve from constant flux) is at 685.014 sec as shown in Figure 3. Fitting the 685.014 sec peak with a Gaussian returns a best period of  $685.0144 \pm 0.0054$  sec. The side bands are primarily artifacts of the alias period from the observation gaps.

For comparison with historical results, we folded the light curve of each observation by the ephemeris from Tan et al. (1991).

$$T_N^{max} = HJD2442803.63544 + (685.0118/86400) \times N, \quad (1)$$

where  $N$  is the cycle count. The phase corresponds to the maximum of the sinusoidal fit of

each folded light curve. A typical folded light curve is shown as Figure 4. Figure 5 shows the phases of the RXTE 1996-1997 observations. The phase of maximum flux are scattered around -0.2 with  $\sim 0.061$  (rms) phase jitter.

To update the ephemeris, we appended the mean arrival times from the RXTE observations to the historical results from SAS-3 (Morgen et al. 1988), Ariel V (Smale et al. 1987), Einstein (Morgan et al. 1988), Tenma (Sansom et al. 1989), EXOSAT<sup>1</sup> (Stella, Priedhorsky and White 1987), Ginga (Sansom et al. 1989, Tan et al. 1991 and van der Klis et al. 1993a) and ROSAT (van der Klis et al. 1993a,b). The phase (or arrival time offset) errors, however, need to be re-estimated. Van der Klis et al. (1993b) discovered the phase shifts about 0.038 in the three ROSAT observations in 1991 and 1993, and the historical phase jitter  $\sim 0.050$  around the best fit linear ephemeris. For the RXTE data in this paper, we found the phase jitter is  $\sim 0.061$  ( $=0.00048$  d). Therefore, an additional 0.061 phase error was quadratically added to the historical data. For the RXTE data, we weighted-averaged the phases from each observation for the 1996 and 1997 datasets separately. We calculated the mean phases errors from quadratically adding the 0.061 phase jitter to the average phase errors from a sinusoidal fit of the folded light curves. The resulting mean phases are  $-0.20259 \pm 0.0613$  and  $-0.20352 \pm 0.0612$  for the 1996 and 1997 datasets respectively. The mean arrival time for the average phases of two datasets were obtained from the expected flux maxima of the mid observation times of the observation windows, that is

$$T_{mean} = T_0 + P_{fold} \times (N_{mid} + \phi_{ave}) \quad (2)$$

where  $T_0 = HJD2442803.63544$ ,  $P_{fold} = (685.01180/86400)$  d,  $N_{mid}$  is the cycle number closest to the mid time of the dataset and  $\phi_{ave}$  is the mean phase for the 1996 and 1997 observations.

The period derivative can be obtained from a quadratic fit

$$\Phi = \Phi_0 + \frac{\Delta P}{(P_{fold})^2}t + \frac{1}{2} \frac{\dot{P}}{(P_{fold})^2}t^2 \quad (3)$$

We applied linear ( $\dot{P} = 0$ ) and quadratic fits to the data. Both fits give acceptable results –  $\chi^2=12.47$  (d.o.f.=21) for linear fit and  $\chi^2=6.96$  (d.o.f.=20) for quadratic fit. However, the F-test (Bevington 1992) shows that  $F(\nu_1=\Delta\nu=1; \nu_2=20)=15.83$  for linear and quadratic fits. This implies that the quadratic fit is better than the linear fit at the  $\sim 99.99\%$  confidence

---

<sup>1</sup>Arrival time errors of 0.0002 d were quadratically added, see van der Klis et al. (1991a)

level. Thus, the quadratic ephemeris is still required.

From the quadratic fit of the data (Figure 6), we obtained  $\dot{P} = (-7.54 \pm 3.21) \times 10^{-13}$  sec/sec or  $\dot{P}/P = (-3.47 \pm 1.48) \times 10^{-8} \text{ yr}^{-1}$ , which is consistent with the value found by van der Kils et al. (1993b). The quadratic ephemeris<sup>2</sup> can be written as

$$T_N = HJD(2442803.63564 \pm 2.2 \times 10^{-4}) + (685.0119 \pm 1.02 \times 10^{-4})/86400 \times N \\ + (-2.99 \pm 1.27) \times 10^{-15} \times N^2 \quad (4)$$

Tan et al. (1991) showed that the 685 sec modulation phases are well fitted by a period of  $\sim 8.5 \pm 0.2$  yr sinusoidal curve from the 1976-1989 observation results. The period may be real or an artifact from the observation gap between 1981 and 1984 (Tan et al. 1991). To clarify the ambiguity, we used the constant-sinusoidal, linear-sinusoidal, and quadratic-sinusoidal models to fit the phases from all the 1976-1997 observations near the 8.5 yr period. The  $\chi^2$  minimum fit results for the three different models are listed in Table 1. Although the linear-sinusoidal and the quadratic-sinusoidal models gave smaller reduced  $\chi^2$  values than the quadratic model, the fitted amplitudes for both cases were only  $\sim 0.05$  (modulation period  $\sim 6.5$  yr), less than the 0.06 phase jitter. Therefore, there is no significant long-term phase periodic modulation of period  $\sim 6$ -8 years and the  $\sim 6.5$  year “period” is highly likely to be an artifact from the phase jitter and the observation gaps between 1976 SAS-3 and 1985 EXOSAT ( $\sim 3500$  d, 1.5 period), 1985 EXOSAT and 1989 Ginga ( $\sim 1300$  d, 0.5 period), and the 1989 Ginga and 1991 ROSAT ( $\sim 1400$  d, 0.5 period) observations.

In explaining the discrepancy between the positive period derivative predicted by the standard scenario vs. the negative observed  $\dot{P}$ , van der Klis et al. (1993b) demonstrated that the negative phase shift could be due to a long-term variation of the disk size. The proposal can be tested by looking for a dependence of orbital phase on  $\dot{M}$  (van der Klis et al. 1993b), or  $L_x$ . We compared the 11 minute modulation phases from the 1996-1997 the RXTE observations and the simultaneous count rates from the RXTE All Sky Monitor (except February 9 1997 observation which has no All Sky Monitor data). The linear correlation coefficient is only 0.17, which implies that the uncorrelated probability is about

---

<sup>2</sup>The small offset due to leap seconds was ignored in our data analysis. The offset is about 16 seconds from zero phase epoch (JD2442803) to end of observations (September 9 1997=JD2450701). If we assume that the offset drifts linearly with time (first order approximation), this systematic effect will give only  $1.6 \times 10^{-5}$  sec offset in the second term of eq. (4). It is much smaller than the error ( $1.02 \times 10^{-4}$  sec) from quadratic fit. The periodic systematic effect due to the difference between the heliocentric time and the barycentric time ( $\sim 2.5$  sec, mainly determined by the position of Jupiter) was also neglected.

70%. Therefore, no significant correlation between binary orbital phases and luminosities is observed. Further considerations about the phase shift are given in section 4.

### 3.2. Possible Period Side Bands

Grindlay (1986, 1988) suggested that the period of  $\sim 176$  d long-term modulation of 4U 1820–30 (PT84) may be due to a hierarchical triple companion star (captured by the compact binary in the high density cluster core) which modulates the eccentricity of the inner binary at a long-term period  $P_{long} = KP_{outer}^2/P_{inner}$ , where  $P_{inner}$  and  $P_{outer}$  refer to the binary period and the orbital period of the third companion and  $K$  is a constant of order unity which depends on mass ratios and relative inclinations (Mazah and Shaham 1979). Under the triple model, with 176 d long-term modulation and 685 sec binary orbital period, the theoretical orbital period of the third star in the 4U 1820–30 system would be  $\sim 1.1$  d (for  $K \simeq 1$ , however, factors of 2 smaller or larger periods for the triple companion could be accommodated for differing inclination). If 4U 1820–30 is a triple system, the 685 sec modulations would be affected by such a period and the beat side bands should appear near the peak of the power spectrum. We considered the binary motion around the center of mass of triple system. For the third companion star of mass  $\sim 0.5M_{\odot}$  (approximate maximum allowed by the optical counterpart) and  $\sim 1.1$  d orbital period, the radius of the binary motion relative to the center of mass of triple system is only  $\sim 3.4 \sin i_3$  light-second, where  $i_3$  is the inclination angle of the orbit of triple companion. In other words, the observed  $\sim 1.1$  d period phase modulation amplitude is no more than  $5 \times 10^{-3}$ . Although the phase variation from the binary motion may be too small to be observed, the third companion star could still affect the light curve in other ways. If, for example, the third companion star makes the 11 minute modulation amplitude change,  $\sim 1.1$  d beat side bands<sup>3</sup> amplitudes may be detectable in the Fourier spectrum.

To search possible side bands, we considered only the 1996 October 26 to 30 light curves because the observation gaps for the 1997 observations were too significant. To further minimize the observation windows (from observation gaps and Earth occultation), a one-dimensional CLEAN algorithm described by Roberts, Lehar & Dreher (1987) was

---

<sup>3</sup>The beat side band periods  $P_{beat} = (1/P_{inner} \pm n/P_{outer})^{-1}$  where  $n$  is positive integer and  $P_{inner}$  and  $P_{outer}$  are the binary (11 minutes) and third star period ( $\sim 1.1$  d), respectively. The first harmonic ( $n=1$ ) beat side band periods are thus 689.97 seconds ( $f=1.45 \times 10^{-3}$  Hz) and 680.10 seconds ( $f=1.47 \times 10^{-3}$  Hz). The apparent sideband peak in the top plot of Figure 7 are tantalizing but probably due to the  $\sim 1$  d spacing between successive observations. A longer continuous observation would be required to remove these alias peaks.

applied to convert for the unequally spaced observations. We searched an arbitrary wide frequency range between  $1.38 \times 10^{-3}$  Hz ( $P=724.6$  sec) and  $1.55 \times 10^{-3}$  Hz ( $P=645.2$  sec) with amplitudes greater than  $2\sigma$  significance. The search results are shown as Figure 7. Only one primary peak is observed. The peak has an amplitude of  $2.42 \pm 0.26$  cts/sec and a period of 685.120 sec. There are no other significant side bands beside this primary peak.

### 3.3. $\sim 176$ Days Modulation

The 1-day average binned light curve for the RXTE ASM data (see Figure 2) shows a clear modulation with relatively rapid rise and slow fall in count rate with a  $\sim 176$  d period. The count rate varies from 5 cts/sec to 35 cts/sec (see Figure 2) throughout each cycle. “Inter dips” were also observed between 1st-2nd, 4th-5th, 5th-6th and 6th-7th minima of the RXTE ASM light curve (minimum cycle count indices are marked on the bottom plot of Figure 2).

PT84 reported the 4U 1820–30 long-term modulation period to be  $176.4 \pm 1.3$  d. However, the ephemeris from PT84 ( $T_{min} = JD2442014.5 + (176.4 \pm 1.3) \times N$ ) does not match the EXOSAT 1985 August 19/20 4U 1820–30 low state observation (Haberl et al. 1985) where the expected minimum (by ephemeris from PT84) was offset by 48 days. A similar discrepancy was found in the data from the Ginga all sky monitor (delayed by  $\sim 50$  d, Sansom et al. 1989, S. Kitamoto, private communications). The light curve of the RXTE ASM data also shows a  $\sim 0.45$  (80d) phase shift (see top plot of Figure 2). The inconsistency may be caused by an incorrect ephemeris (phase zero epoch, period or both) or a period drift.

To obtain the best period to describe the 4U 1820–30 RXTE ASM light curve, we first applied a fast Fourier transformation (FFT). However, because the observation window is only a brief  $\sim 8.8$  cycles (1576 days), the FFT frequency resolution,  $\delta f = 1/(1576\text{d}) = 0.233$  cycle per year, yields the period resolution near 176 d of  $\delta P \approx P^2 \times \delta f = 19.8$  d, which is too coarse for  $\sim 176$  d period modulation. Therefore, the interpolated Fourier transformation (Middleditch, Geich and Kulkarni 1993) was applied to further determine the best period. The FFT is only able to show amplitudes of the “integer” frequencies ( $f_n = n/T$  where  $n$  is an integer and  $T$  is the total time of the data) whereas the interpolated Fourier may show the amplitude of “non-integer” frequencies ( $f_r = r/T$ , where  $r$  is any real number). The non-integer amplitude  $A_r$  can be estimated from the locally neighboring Fourier amplitudes as

$$A_r \sim \sum_{l=[r]-m}^{[r]+m} A_l e^{-i\pi(r-l)} \frac{\sin(\pi(r-l))}{\pi(r-l)} \quad (5)$$

where  $m$  is integer and  $[r]$  denotes the nearest integer of  $r$ . The uncertainty of peak frequency

$$\sigma_f = \frac{3}{\pi \alpha T \sqrt{6P_0}} \quad (6)$$

where

$$\alpha = \frac{1}{\pi T} \sqrt{-\frac{3}{2P_0} \frac{\partial^2 P}{\partial f^2}} \quad (7)$$

$P_0$  the peak power, and  $T$  is the length of the observation window (Middleditch, Geich and Kulkarni 1993).

We chose  $m=2$  and the resolution of  $r$  to be 0.1. The interpolated Fourier transformation spectrum is shown in the bottom plot of Figure 8. The peak amplitude was observed at  $f=2.130$  cycle/yr with a value of 4.506 cts/sec. The frequency uncertainty from eq. (6) and eq. (7) is 0.0240 cycle/yr where the second derivative in eq. (7) is estimated by the quadratic fit around the peak of the power spectrum. Therefore, the best 4U 1820–30 long-term modulation period for the RXTE ASM data is  $171.39 \pm 1.93$  d. Furthermore, the  $\chi^2$  period searching method gave the best period of 171.23 d ( $\pm 7.36$  d), close to the interpolated Fourier transformation result.

The RXTE ASM light curve, derived by folding at a period of 171.39 d (see Figure 9), shows that the minimum closest to the mid of observation is at JD2450907.96 and  $\pm 0.07$  (rms) phase jitter (or  $\pm 12$  d). The best linear ephemeris to describe the intensity minimum of the RXTE ASM light curve (hereafter local ephemeris) can be written as

$$T_{min}^{RXTE} = JD2450907.96 \pm 12.00 + (171.39 \pm 1.93) \times N. \quad (8)$$

To obtain the best linear ephemeris for the intensity minimum in the RXTE ASM light curve and historical data, we assigned an uncertainty  $\pm 12$  d (from 0.07 phase jitter obtained from the RXTE ASM light curve) to the minimum time reported by PT84 (JD2442014.5). Combined with intensity minimum times observed by the Ginga all-sky monitor (JD2446822 $\pm$ 26, S. Kitamoto, private communications) and RXTE ASM data, the linear fit yields the best historical ephemeris of

$$T_{min} = JD2450909.90 \pm 11.66 + (171.033 \pm 0.326) \times N. \quad (9)$$

The expected intensity minimum times from eq. (9) vs. the RXTE ASM light curve are shown as the bottom plot of Figure 2. An independent check on the ephemeris may be derived from timing of x-ray burst activity. Stella, Kahn and Grindlay (1984 and references therein) reported that no bursts are detected in the high state, which implies that the “burst phase” should be near phase zero. Table 2 lists the observation dates with bursts being detected and the phases of these days. No burst phase folded by eq. (9) exceeded the range  $\pm 0.13$  ( $\pm 23$  d). This indicates that the long-term modulation period of 4U 1820–30 is close to 171.033 d and stable over  $\sim 30$  years.

To estimate the period derivative (or its upper limit), we suppose the minimum times ( $T_N$ ) obey a quadratic ephemeris (for small  $\dot{P}$ )

$$T_N = T_0 + P_0 N + \frac{1}{2} P_0 \dot{P} N^2, \quad (10)$$

where  $N$  is cycle count index. Taking the phase zero epoch  $T_0$  to be that in eq. (8) (JD2450907.96), since the cycle numbers are small for RXTE intensity minima (from -4 to 4), the quadratic term in eq. (10) can be neglected. Eq. (10) is reduced to a linear ephemeris equal to the local ephemeris (i.e. eq. (8)). The phases of historical data (Vela 5B and Ginga) folded by eq. (8) should be due to the period derivative

$$\Phi = \frac{1}{2} \frac{\dot{P}}{(P_0)^2} \Delta t^2, \quad (11)$$

where  $\Delta t$  is time difference between minimum time and  $T_0$ . Applying eq. (8) to historical data, we found no significant period derivative. The  $2\sigma$  (90%) confidence level upper limit for the change in 171 d period is  $|\dot{P}| < 1.03 \times 10^{-4}$  days per day (= 0.038 days per year) or  $|\dot{P}/P| < 2.20 \times 10^{-4}$  yr $^{-1}$ . This stable long-term modulation is consistent with 4U 1820–30 being a hierarchical triple system with a  $\sim 1.1$  d period companion.

#### 4. DISCUSSION

The observed negative period derivative from the 4U 1820–30 RXTE 1996-1997 observations combined with all the historical data is consistent with the previous conclusions proposed by Tan et al. (1991) and van der Klis et al. (1993a,b). The decreasing 685 sec

period deviates from the positive  $\dot{P}$  ( $\dot{P}/P > 8.8 \times 10^{-8} \text{ yr}^{-1}$ ) predicted by the standard scenario (Rappaport et al. 1987). Tan et al. (1991) suggested that the discrepancy is probably caused by the acceleration of the binary star by the gravitational potential of the globular cluster. On the other hand, by analyzing the theoretical minimum of the period derivative, van der Klis et al. (1993a) found that the gravitational acceleration by the globular cluster is not enough to explain the observed results even if the line of sight is very close to the line connecting the binary with the center of the cluster at the projected separation  $4 \pm 1$  arcsec.

However, King et al. (1993) measured the NGC6624 cluster center with the HST Faint Object Camera (FOC) and discovered that 4U 1820–30 is 0.66 arcsec from the cluster center. For an assumed distance of 6.4 kpc (Vacca et al. 1986, Haberl and Titarchuk 1995), this is equivalent to only 0.02 pc (projected) from the core. Using the model proposed by van der Klis et al. (1993a), the maximum gravitational acceleration along the line of sight could be  $a/c = 2.5 \times 10^{-15} \text{ sec}^{-1}$ . Combining the period derivative derived in section 3.1 and its value from the standard scenario, we determined the acceleration along the line of sight to be  $a/c = 3.9 \times 10^{-15} \text{ sec}^{-1}$ , only  $\sim 50\%$  larger than the maximum value. Therefore, given the uncertainties both in  $\dot{P}$  and the cluster acceleration (i.e. center and mass model), gravitational acceleration by the globular cluster is still a possible explanation for the negative period derivative (also see King et al. 1993).

Another potential explanation of the negative period derivative (or, negative phase shift) was proposed by van der Klis et al. (1993b). The 685 sec intensity modulation of the 4U 1820–30, as for the dipping sources, is probably caused by the occultation by the accretion stream of the vertical structure at the edge of the accretion disk (Stella, Friedhorsky and White 1987; Morgan et al. 1988; Sansom et al. 1989; van der Klis et al. 1993b). The azimuth point of impact depends on the disk size. The bulge on the disk rim could shift by as much as  $\sim -120^\circ$ , larger than the observed phase shifts of  $\sim -72^\circ$  ( $-0.2$  phase; the approximate value needed to account for the negative  $\dot{P}$ ). However, if we consider only the standard scenario,  $\dot{P}/P \sim 8.8 \times 10^{-8} \text{ yr}^{-1}$ , the phase shift due to the period change is expected to be  $\sim +0.75$  from the 1976 SAS3 to the 1997 RXTE observations. This result implies that the total bulge phase shift is  $\sim -0.95 (-350^\circ)$ . The bulge is unlikely to have such a large phase shift. Furthermore, the disk size should be highly correlated with the accretion rate and, of course, the luminosity  $L_x$ . As discussed in section 3.1, no significant correlation between orbital phase and luminosity (171 d variation) is found in the RXTE 1996-1997 data. We hence conclude that the negative phase shift is unlikely to be caused by a variation of the disk size.

In this paper, we derived the long-term modulation period and showed from the ephemeris (eq. (9)) that the 4U 1820–30 bursts are only observed in the low state. By re-analyzing the

historical data as well as tabulated burst activity time, we derived a period  $P=171.033\pm0.326$  d and a limit on  $|\dot{P}| < 1.03 \times 10^{-4}$  days per day. The high correlation between the burst activity and the luminosity suggests that the 171 d modulation is stable and indeed an intrinsic luminosity change rather than an extrinsic periodic obscuration. This luminosity modulation and (primarily) its long-term stability supports earlier suggestions for a hierarchical triple companion. The mass transfer rate is very sensitive to the Roche lobe radius, which is proportional to the inner binary separation. A hierarchical companion third star will induce an eccentricity variation in inner (11 minutes) binary with period  $P_{long} = KP_{outer}^2/P_{inner}$  (Mazeh and Shaham, 1979). When the minimum separation of the inner binary is small, the mass transfer rate and luminosity changes are enhanced. The triple model to 4U 1820–30 system implies a  $\sim 1.1$  d period third companion is responsible for the 171.033 d long-term intensity modulation. The triple companion star affects the orbital motion of the inner binary through beats of 685 sec binary period and  $\sim 1.1$  d companion star orbital period. Our RXTE observations were not sensitive to this because of both data sampling ( $\sim 1$  d observation gaps) and the small amplitude expected. An additional test of the triple model could be conducted by a continuous, or optimally sampled long ( $\gtrsim 3$ -10 d) observation of 4U 1820–30 to measure the small ( $\sim 3.4 \sin i_3$  light-second, see section 3.2) phase shifts, or the possible modulation side bands (Figure 7) without 1 d sampling alias effects.

The authors thank S. Kitamoto for invaluable assistant with the Ginga data, RXTE-GOF for help with RXTE data analysis, and the HEASARC for archival RXTE ASM data. This work was supported in part by NASA grant NAG5-3293 and NAG5-7393.

## REFERENCES

- Anderson, S. F., et al. 1997, ApJ, 482, L69
- Bevington, P. R. 1992, Data Reduction and Error Analysis for the Physical Sciences (New York: McGraw-Hill)
- Bloser, P. F., Grindlay, J. E., Kaaret, P., Zhang, W., Smale, A.P., Barret, D. 2000, ApJ, 542, 1000
- Canizares, C. R. & Neighbours, J. E. 1975, ApJ, 199, L97
- Clark, G. W., et al. 1976, ApJ, 207, L105
- Clark, G. W., et al. 1977, MNRAS, 179, 651
- Grindlay J. E., et al. 1976, ApJ, 205, L127
- Grindlay J. E., et al. 1984, ApJ, 282, L13

- Grindlay J. E. 1986, in *The Evolution of Galactic x-ray Binaries*, J. Trumper, W. Lewin and W. Brinkman, eds., Nato ASI Series, Vol. 167, p. 25
- Grindlay, J. E. 1988, in *IAU Symposium, Globular Cluster System in Galaxies*, ed. J. E. Grindlay and A. G. Davis Philip (Dordrecht: Reidel), p. 347
- Haberl, F., et al. 1987, *ApJ*, 314, L266
- Haberl, F. and Titarchuk, L. 1995, *A&A*, 299, 414
- Hasinger, G. & van der Klis, M. 1989, *A&A*, 225, 79
- Kaaret, P., et al. 1999, *ApJ*, 520, L37
- King, I. R., et al. 1993, *ApJ*, 413, L117
- Mazeh, T. & Shaham, J. 1979 *A&A*, 77, 145
- Middleditch, J., Deich, W. & Kulkarni, S. 1993, in *Isolated Pulsar* (Cambridge University press), Van Riper, Epstein and Ho (eds), p. 372
- Morgan, E. H. Remillard, R. A. & Garcia, M. R. 1988, *ApJ*, 324, 851
- Priedhorsky, W. & Terrell, J. 1984, *ApJ*, 284, L17
- Rappaport, S., et al. 1987, *ApJ*, 322, 84
- Roberts, D. H., Lehar, J. & Dreher, W. 1987, *Astron. J.*, 93, 968
- Sansom, A. E., et al. 1989, *PASJ*, 41,591
- Smale, A. P., Mason, K. O. & Mukai, K. 1987, *MNRAS*, 225, 7
- Smale, A. P., Zhang, W. & White, N. E. 1997, *ApJ*, 483, L119
- Stella, L. Kahn, S. M., and Grindlay J. E. 1984, *ApJ*, 282, 713
- Stella, L., Peirdhorsky, W. & White, N. E. 1987, *ApJ*, 312, L17
- Stella, L., White, N. E. & Peirdhorsky, W. 1987, *ApJ*, 315, L49
- Tan, J., et al. 1991, *ApJ*, 374, 291
- Vacca, W.D., Lewin, W. H. G., & van Paradijs, J. 1986, *MNRAS*, 220 339
- van der Klis, M., et al. 1993a, *MNRAS*, 260, 686
- van der Klis, M., et al. 1993b, *A&A*, 279, L21
- Wijnands, R., van der Klis, M. & Rijkhorst, E. 1999, *ApJ*, 512, L39
- Zhang, W., et al. 1998 *ApJ*, 500, L171

Fig. 1.— Light curve of 4U 1820–30 (6.84-19.84 keV) observed by RXTE PCA on 1996 October 28/29.

Fig. 2.— The 4U 1820–30 light curve observed by RXTE All-Sky Monitor from 1996 January 11 to 2000 March 2. The dashed lines are the expected minimum intensity times for the ephemeris from PT84 (top) and ephemeris of eq. (9) in section 3.3 (bottom).

Fig. 3.— The result of  $\chi^2$  folded period searching of RXTE PCA 1996-1997 observation. The Gaussian fit of the peak near 685.01 sec yields a best period of  $685.0144 \pm 0.0054$  sec.

Fig. 4.— The folded light curve of the observation on 1997 September 10 folded by eq. (1) and with the dc flux subtracted. The maximum of sinusoid fit is at about phase 0.8 (or -0.2). Inter-dip is observed at phase 0.5 to 0.6.

Fig. 5.— The phases of 4U 1820–30 RXTE PCA 1996-1997 observation. The mean fluctuation of the phases is about 0.061.

Fig. 6.— The phases of 4U 1820–30 11 minutes modulation from 1976-1997 observation folded by the ephemeris of eq (1). The dashed line represents the best quadratic fit result.

Fig. 7.— The raw (top) and CLEAN (bottom) Fourier amplitude (i.e. absolute values of the Fourier transformation) spectra of RXTE 1996 October observations. The upper amplitude limit for the CLEAN spectrum is 0.52 cts/sec ( $2\sigma$ ). There is no clear side band beside the peak; therefore, the side bands in the raw spectrum are likely artifacts from  $\sim 1$  d observation gaps.

Fig. 8.— Raw FFT spectrum (top) and interpolated Fourier spectrum (bottom) of the 4U 1820 RXTE ASM light curves.

Fig. 9.— The 4U 1820–30 RXTE ASM light curve folded by the local ephemeris (eq. (8)).

Table 1. Phase modulation fit results

| Model            | Reduced $\chi^2$ | Period from<br>sinusoidal fit (day) | Amplitude from<br>sinusoidal fit |
|------------------|------------------|-------------------------------------|----------------------------------|
| L <sup>a</sup>   | 0.594            | -                                   | -                                |
| Q <sup>b</sup>   | 0.349            | -                                   | -                                |
| C+S <sup>c</sup> | 0.782            | $2978.3 \pm 140.7$                  | 0.0965                           |
| L+S <sup>d</sup> | 0.315            | $2475.9 \pm 224.8$                  | 0.0567                           |
| Q+S <sup>e</sup> | 0.223            | $2368.9 \pm 267.0$                  | 0.0446                           |

<sup>a</sup>Linear model

<sup>b</sup>Quadratic model

<sup>c</sup>Constant + sinusoidal model around P=8.5 year

<sup>d</sup>Linear + sinusoidal model around P=8.5 year

<sup>e</sup>Quadratic + sinusoidal model around P=8.5 year

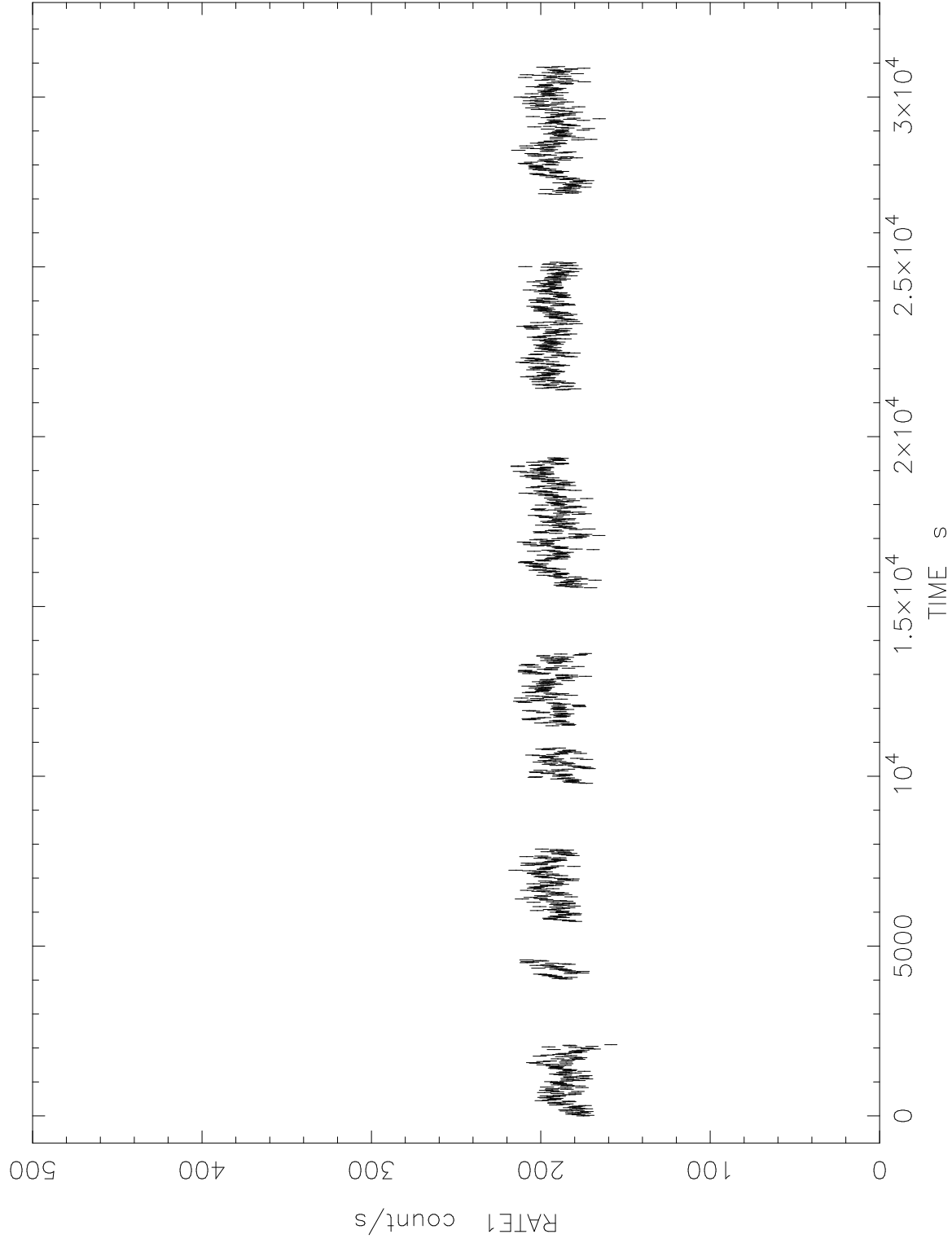
Table 2. X-ray Burst phases

| Observation date<br>(dd/mm/yy) | Observation date<br>(JD) | Phase folded by<br>PT ephemeris | Phase folded by<br>eq. (9) | Reference |
|--------------------------------|--------------------------|---------------------------------|----------------------------|-----------|
| 18/05/75                       | 2442550.5                | 0.039                           | 0.124                      | 1         |
| 28/09/75                       | 2442683.5                | -0.207                          | -0.098                     | 2         |
| 15/03/76 <sup>a</sup>          | 2442852.5                | -0.250                          | -0.110                     | 3         |
| 20/08/85                       | 2446297.5                | 0.280                           | 0.032                      | 4         |

<sup>a</sup>Mid observation date of 1976 March 11.5 to 19.5

References. — (1) Clark et al. 1976; (2) Grindlay et al. 1976; (3) Clark et al. 1977; (4) Haberl et al. 1987

Plot of file 1820.lc.Oct\_28\_96.flc



15-Sep-1999 14:23

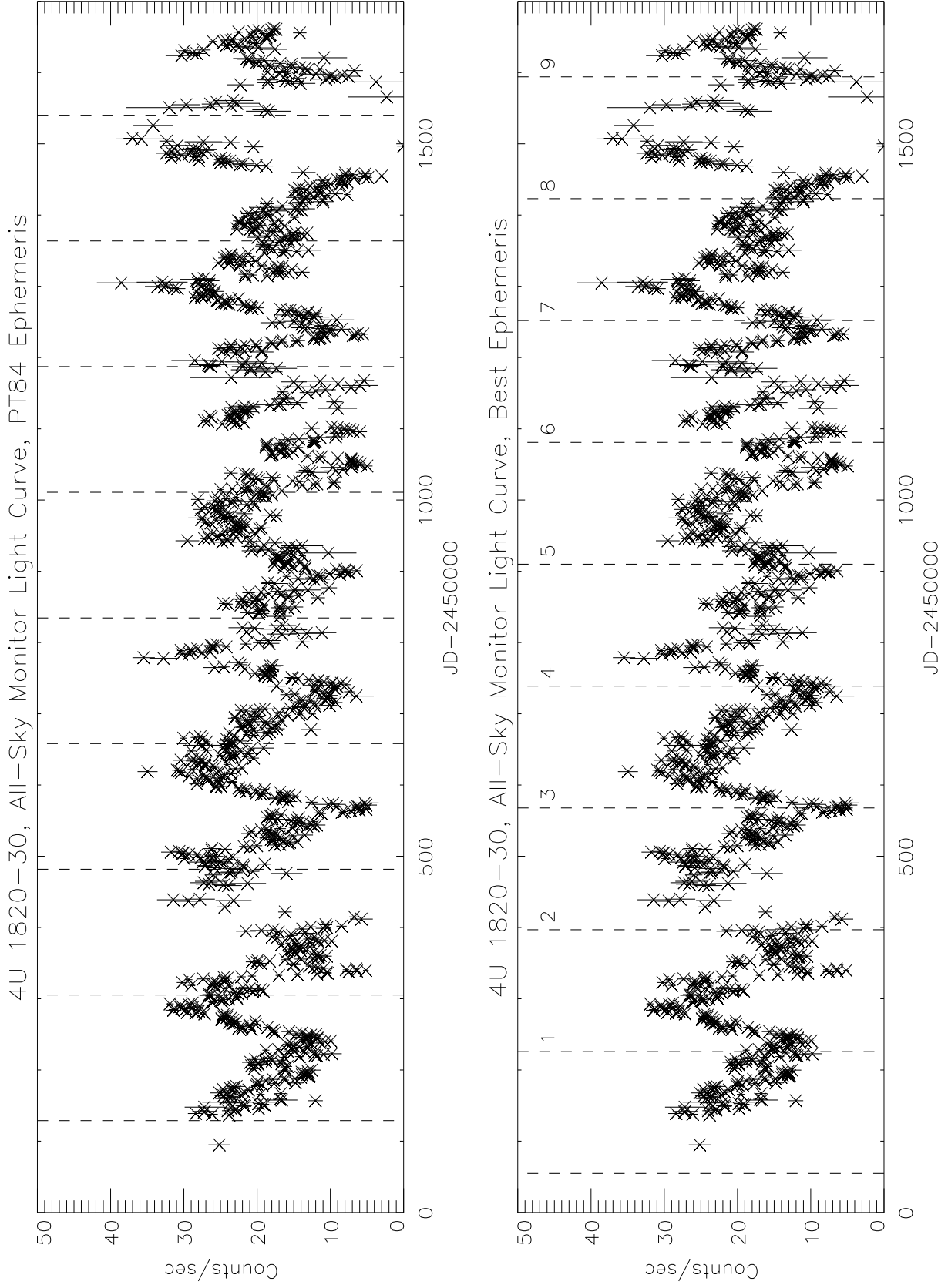


Fig. 2.—

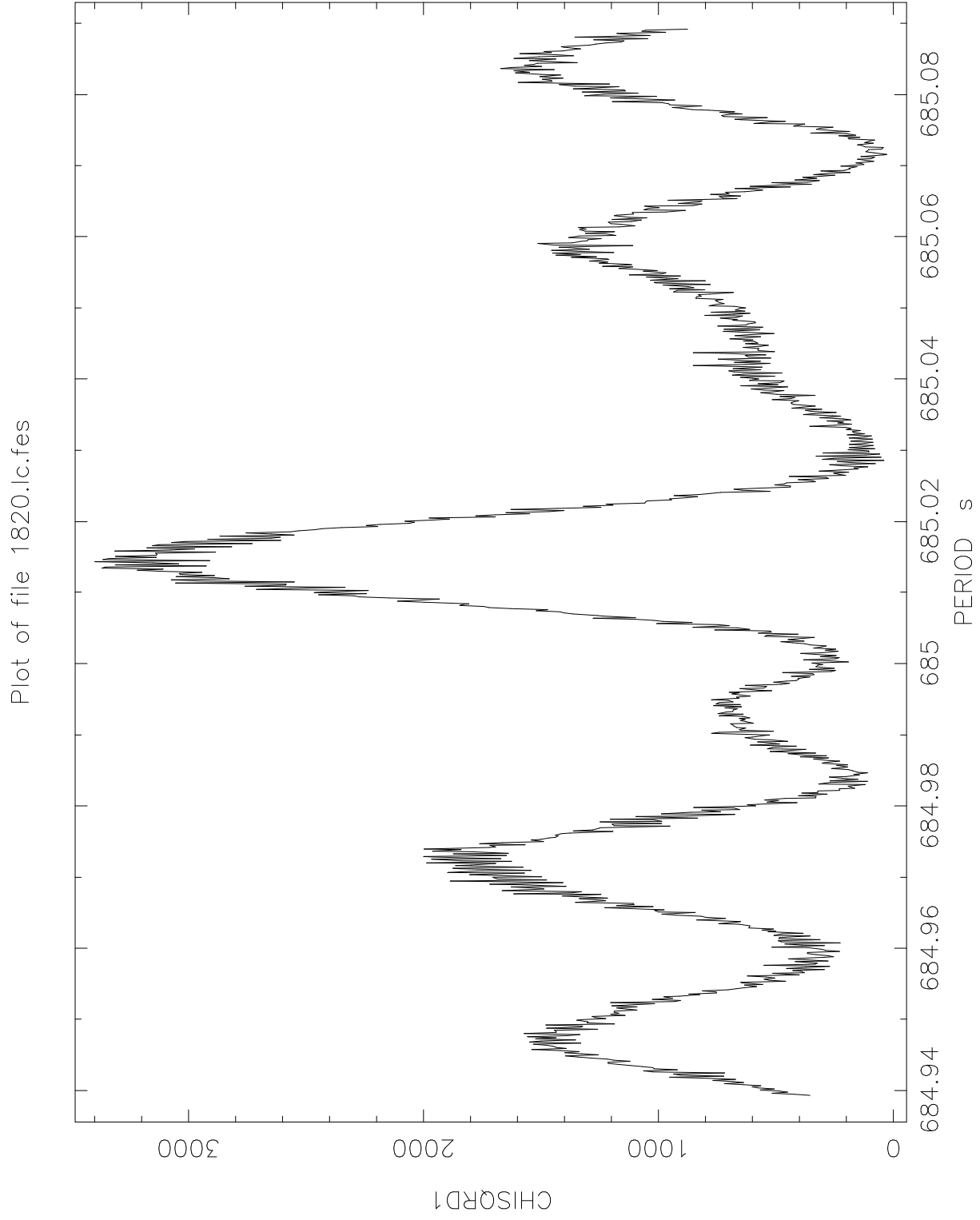
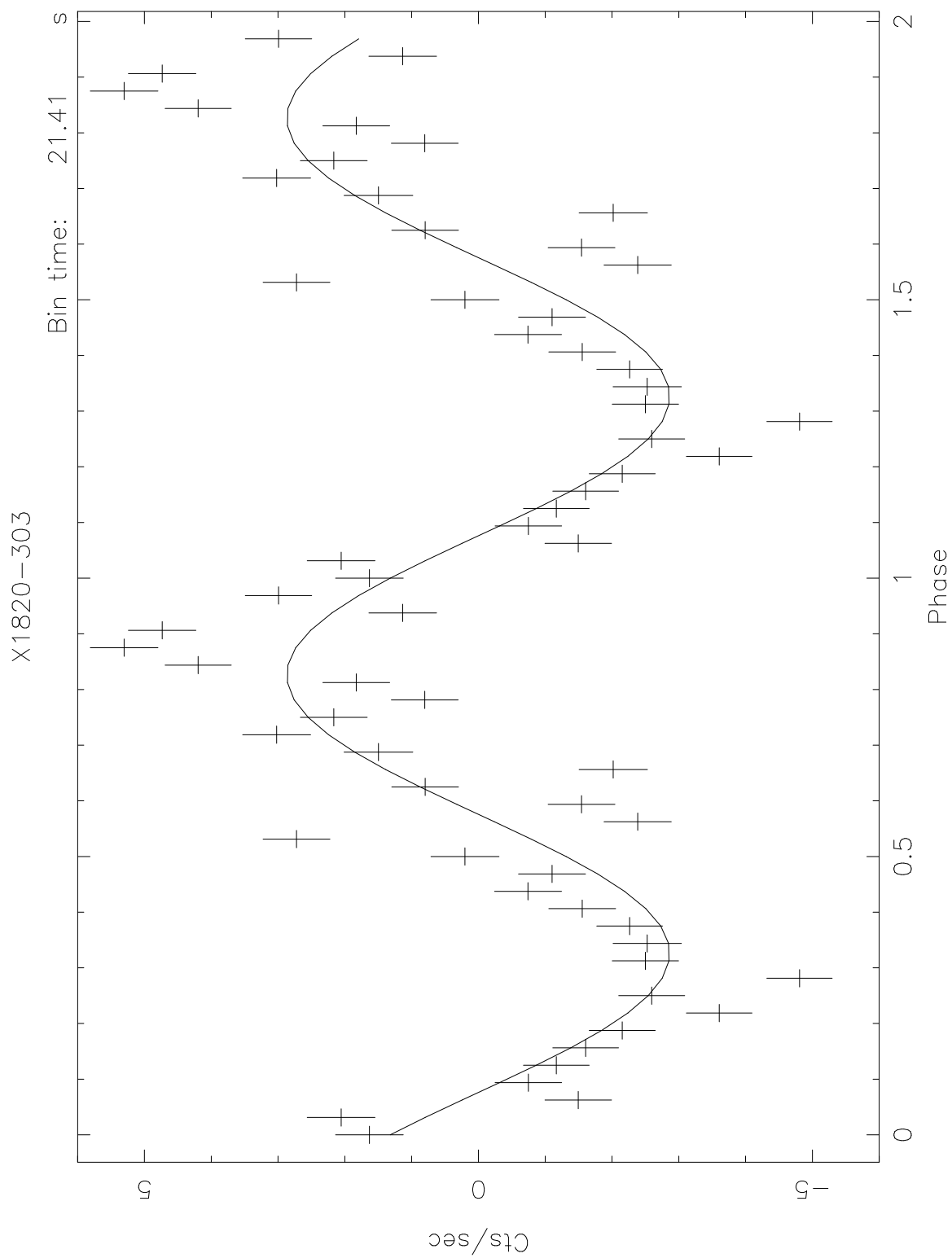


Fig. 3.—

Fig. 4.—



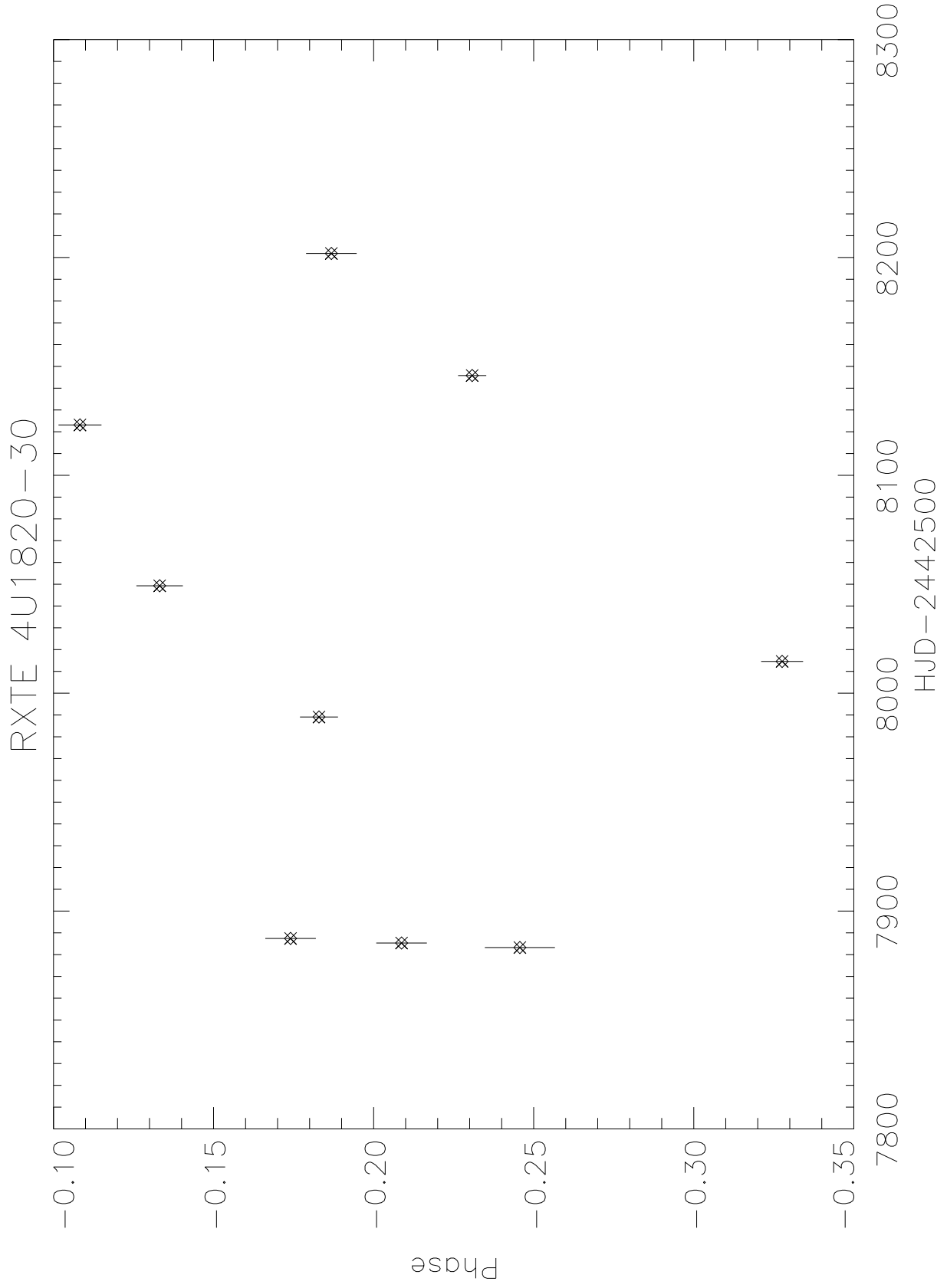


Fig. 5.—

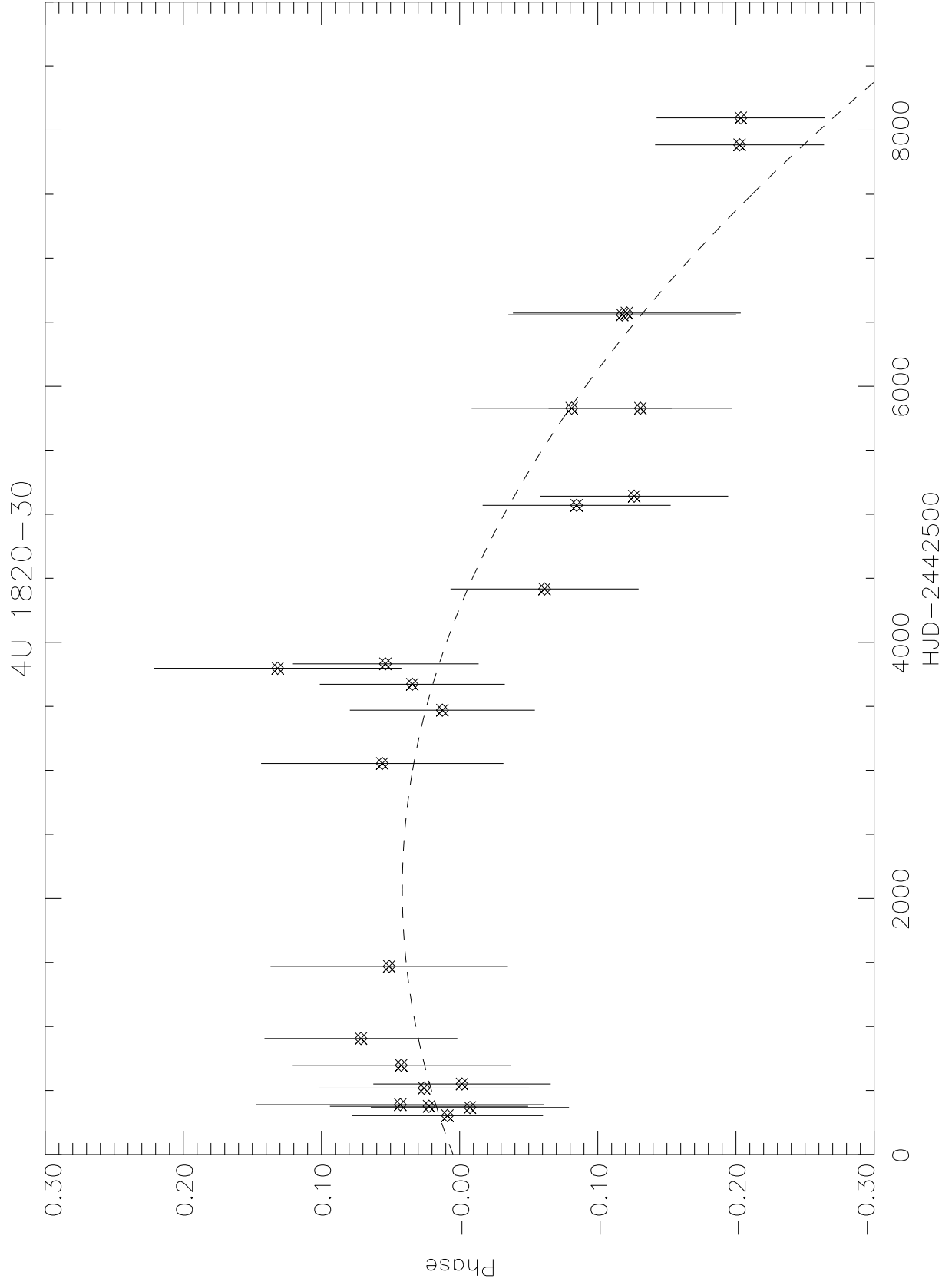
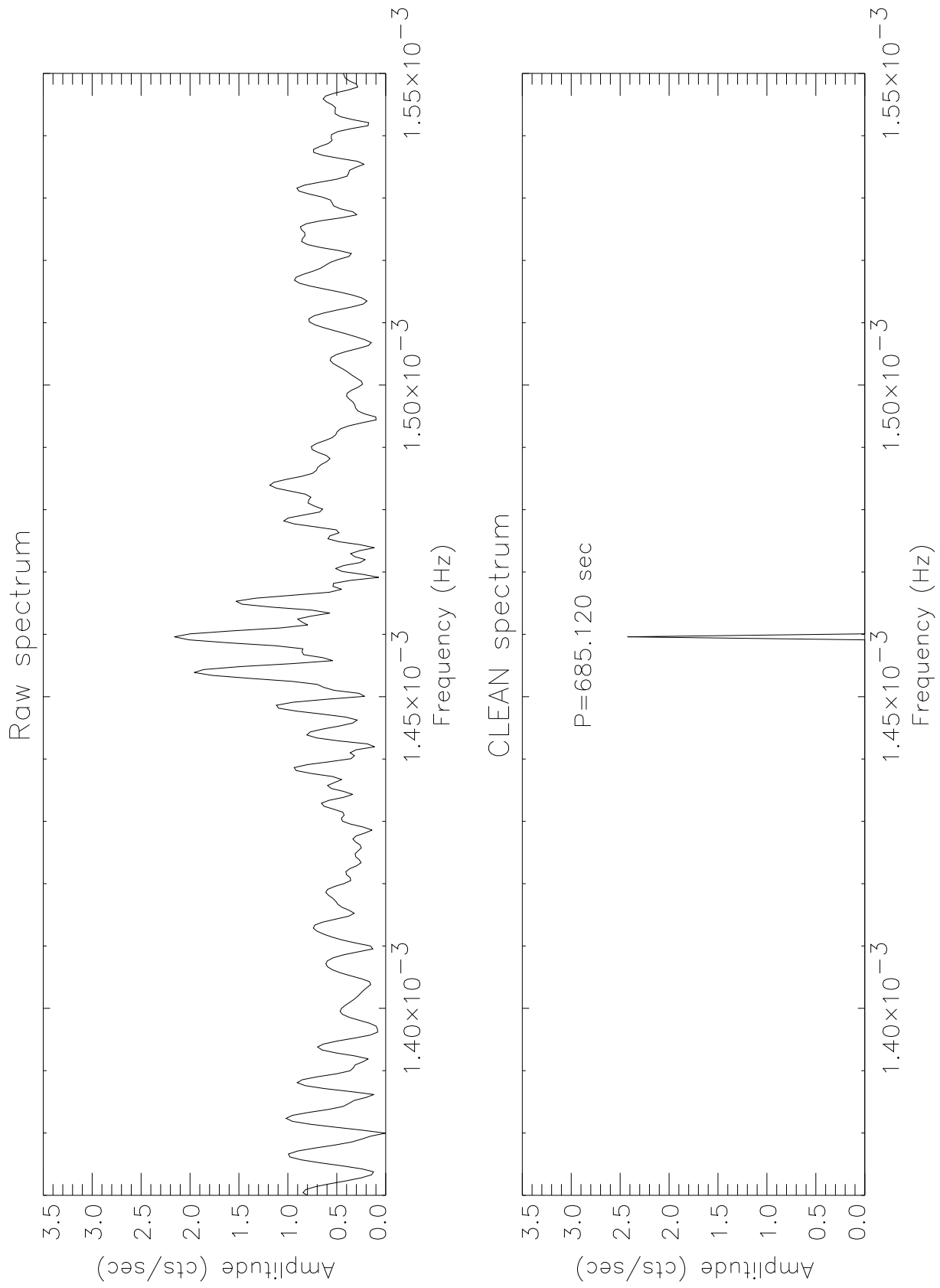


Fig. 6.—

Fig. 7.—



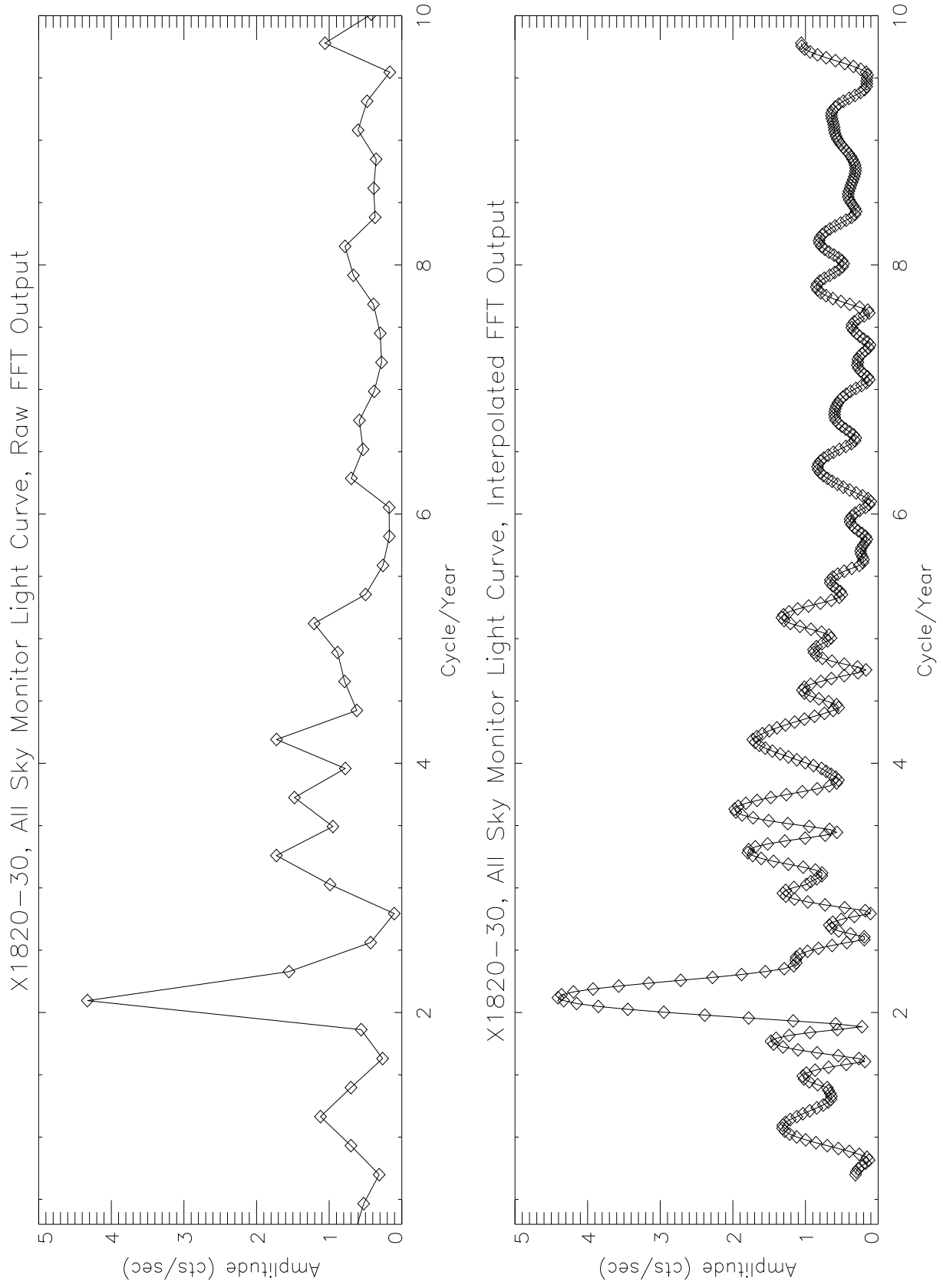


Fig. 8.—

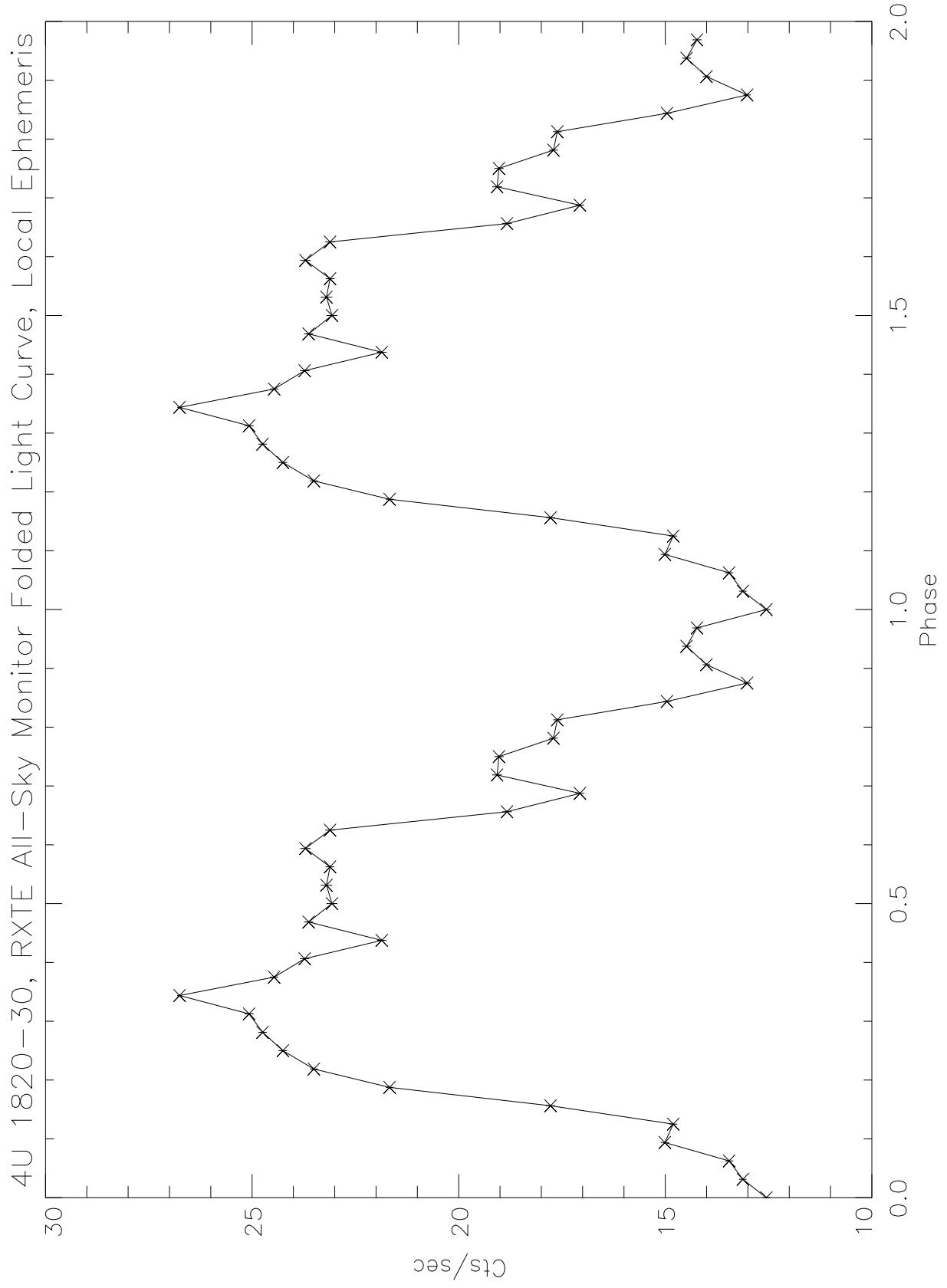


Fig. 9.—